

# A preliminary study of iron isotope fractionation in marine invertebrates (chiton, mollusca) in near shore environments

**Simon Emmanuel<sup>1\*</sup>, Jan A. Schuessler<sup>2</sup>, Jakob Vinther<sup>3</sup>, Alan Matthews<sup>1,4</sup>, and  
Friedhelm von Blanckenburg<sup>2</sup>**

<sup>1</sup>Institute of Earth Sciences, The Hebrew University of Jerusalem, Jerusalem, Israel

<sup>2</sup>Helmholtz Centre Potsdam, German Research Centre for Geosciences GFZ, Section 3.4, Earth  
Surface Geochemistry, Potsdam, Germany

<sup>3</sup>School of Earth Sciences, University of Bristol, Bristol, UK

<sup>4</sup>National Natural History Collections, Institute of Earth Sciences, Hebrew University of Jerusalem,  
Jerusalem, Israel

**\*Corresponding author: [swemmanuel@gmail.com](mailto:swemmanuel@gmail.com)**

## 2 1. INTRODUCTION

3 Iron plays a critical role in controlling biological productivity in the oceans (Martin et al.,  
4 1990; De Baar et al., 1995; Coale et al., 1996), and understanding the biogeochemical cycling  
5 of Fe is therefore key in reconstructing the history of life on Earth. One potentially rewarding  
6 way to reconstruct past marine conditions is to examine variations in the isotopic signature of  
7 iron. Changes to Fe isotope ratios occur due to shifts in redox state, chemical bonding  
8 environment, adsorption properties, and microbial and organic-ligand bonding processes (e.g.,  
9 Matthews et al., 2001; Zhu et al., 2002; Beard et al., 2003a,b; Brantley et al., 2004; Croal et  
10 al., 2004; Welch et al., 2003; Johnson et al., 2005; Teutsch et al., 2005; Crosby et al., 2007;  
11 Matthews et al., 2008), and precise measurements of these isotopes could yield vital  
12 information about geochemical and ecological conditions in both present day and past  
13 environments.

14 While studies have examined isotopic variations of Fe in marine rocks (e.g., Matthews  
15 et al. 2004; Staubwasser et al., 2006; Severmann et al., 2006), marine organisms that  
16 accumulate significant amounts of Fe could also prove to be good environmental recorders.  
17 One group of marine molluscs that might fulfill this role is chitons (Figure 1 a-b). Belonging  
18 to the class Polyplacophora, these molluscs graze on algae on the surface of rocks and other  
19 hard substrates in the near shore coastal environment using radula (or rasping tongue) made  
20 up of teeth impregnated with magnetite and other iron bearing minerals, such as ferrihydrite,  
21 goethite, and lepidocrocite (e.g., Lowenstam, 1962a; Towe and Lowenstam, 1967;  
22 Lowenstam and Kirschvink, 1996; Lowenstam and Weiner, 1989). Due to their high level of  
23 iron accumulation, the Fe isotopic signature of modern chiton radula might be expected to  
24 reflect ambient oceanic environments.

25 However, a number of factors may influence the isotopic composition of Fe  
26 accumulated in chiton teeth at any given location. Being primarily herbivorous, they extract  
27 nutrients from marine algae, which in turn absorb nutrients directly from seawater. As the

28 isotopic composition of Fe in seawater can vary spatially due to variations in the relative  
29 contributions of different sources, including continental runoff, aerosols, hydrothermal fluids,  
30 and oceanic crust alteration (Sharma et al., 2001; Anbar & Rouxel, 2007; Johnson et al., 2008;  
31 Homoky et al., 2012), the isotopic value recorded in invertebrate teeth could therefore change  
32 with geographical location. In addition, utilization by marine organisms and associated  
33 biological fractionation may also play an important role in determining Fe isotope  
34 compositions. Bacteria are known to form isotopically light magnetite during dissimilatory  
35 microbial reduction of Fe(III) oxyhydroxides (Johnson et al., 2005); other organisms, such as  
36 algae and even the chitons themselves, could also fractionate Fe isotopes as a result of  
37 biomineralization processes. Although Fe isotope signatures in higher organisms have been  
38 studied (e.g., Walczyk & von Blanckenburg, 2002; Hotz, 2011), little is currently known  
39 about the natural variation of metal isotopes in marine invertebrates or the influence that  
40 biological fractionation and environmental factors, such as geographical location and diet,  
41 may have on those signatures.

42         Here, in a preliminary study, we examine Fe isotopes in modern marine chitons  
43 collected from different locations in the Atlantic and Pacific oceans to determine the range of  
44 isotopic values that might be encountered and whether or not these isotopic signatures reflect  
45 seawater values. Furthermore, by comparing two different species that were collected from  
46 the same geographical location but have very different feeding habits, we make a *first* attempt  
47 to isolate the potential impact of diet on metal isotopic signatures. While our findings are not  
48 definitive, the small new dataset sheds light on the possible pathways of Fe biogeochemical  
49 cycling in near-shore environments, highlighting important new directions for future research.

50

## 51 **2. METHODS**

52 Ideally, chiton samples would have been obtained from a field campaign that collected  
53 specimens from different locations around the world. However, in this preliminary study such

54 an approach was not feasible, and instead samples were selected from the collections at the  
55 Peabody Museum of Natural History at Yale University. The samples were collected in the  
56 early 1900's and preserved in formalin, which primarily acts as an antimicrobial agent;  
57 although the effect of prolonged exposure of Fe oxides to formalin is not known, we assume  
58 no mineralogical or isotopic changes to have occurred in the samples. A total of 24 individual  
59 chiton specimens representing 5 different species from 4 different geographical locations were  
60 selected for analysis. A summary of the samples is given in Table 1. To represent  
61 high and low latitude sites from the Atlantic Ocean, chitons from Bermuda and New  
62 Brunswick, Canada, were sampled; from the Pacific Ocean, samples from Panama and  
63 Washington State, USA, were selected. In addition, from the Washington locality, two  
64 different species – *Tonicella lineata* and *Mopalia muscosa* that feed on predominantly green  
65 algae and red algae respectively – were selected for comparison. Of the 5 species investigated  
66 in this study, 3 inhabit the eulittoral (intertidal) zone, while 2 are found in the sublittoral  
67 (neritic zone). The eulittoral zone is characterised by tidal activity and extends from the low  
68 tide line to the high tide line leading to periodic dry and flood periods. The sublittoral zone  
69 starts immediately below the eulittoral zone and is permanently underwater. Sunlight  
70 penetrates to the seafloor in the eulittoral zone so that both the eulittoral and sublittoral zones  
71 are within the photic zone.

72         The protocol for sample preparation involved dissection of the chitons to extract the  
73 radula sac containing the magnetite-capped teeth; a magnetic separation technique was used  
74 to separate the radula from the organic matter. A single radula is made of two symmetric rows  
75 of teeth (Figure 1a). The total number and size of teeth of each radula can vary depending on  
76 the species. Here, each isotopic analysis (Table 1) represents a homogenised sample  
77 comprising all teeth of a complete radula for each individual specimen. Due to the small size  
78 of the radula for *Tonicella marmorea* from New Brunswick, the teeth from 8 individual

79 specimens were combined and homogenized to produce one isotopic measurement. One  
80 sample (YPM12739-16) was processed in duplicate, and a total of 18 values are reported here.

81 After separation, the radula were then processed in a clean room facility, where they  
82 were digested using ultrapure concentrated HCl; hydrogen peroxide was also added to remove  
83 any residual organic material. The digested sample solution was evaporated on a hot plate and  
84 re-dissolved in 6M HCl and then passed through chromatographic columns to isolate Fe (Zhu  
85 et al., 2002; Archer & Vance, 2004). Purity of samples and quantitative recovery of iron after  
86 the column separation procedure was verified by inductively coupled plasma - mass  
87 spectrometry (ICP-MS; Agilent 7500cx) analyses. Total Fe amounts ranged from 30  $\mu\text{g}$  to  
88 840  $\mu\text{g}$ . Purity of Fe analyte solutions was found to be better than 99%, which is sufficient for  
89 accurate Fe isotope analyses using the method described below (Schoenberg and von  
90 Blanckenburg, 2005). Noteworthy, efficient separation of Cr and Ni from Fe was achieved,  
91 eliminating spectral interferences of  $^{54}\text{Cr}$  on  $^{54}\text{Fe}$  and  $^{58}\text{Ni}$  on  $^{58}\text{Fe}$  during mass spectrometric  
92 measurements of Fe isotope ratios. The procedure was also tested by processing the reference  
93 material IRMM-014 repeatedly through the same chromatographic separation protocol as the  
94 samples. This method yielded a  $\delta^{56}\text{Fe}$  value for IRMM-014 of  $-0.03 \pm 0.02$  (2SE, n=16),  
95 which is identical with the unprocessed IRMM-014, within the external uncertainty of the  
96 method. Prior to isotope analysis, samples were dissolved in 0.3M  $\text{HNO}_3$  and diluted to about  
97 2  $\mu\text{g}/\text{ml}$  Fe, matching the ion beam intensities ( $\sim 20$  V on  $^{56}\text{Fe}$ ;  $10^{11}\Omega$  amplifier, H cones) of  
98 the bracketing standard (IRMM-014) within 10%. The Fe isotopic analyses were performed  
99 on a total set of 18 chiton samples using a *Thermo Scientific Neptune* multi collector  
100 inductively coupled plasma mass spectrometer (MC-ICP-MS) at GFZ Potsdam in Germany.  
101 The mass spectrometer is equipped with a *Neptune Plus Jet Interface Pump* and an *ESI Apex-*  
102 *Q* desolvating system (without membrane) with a  $\sim 50$   $\mu\text{l}/\text{min}$  PFA nebuliser for sample  
103 introduction. Iron isotope analyses were performed in ‘medium’ mass resolution mode (mass

104 resolving power  $m/\Delta m$  (5%, 95%) > 7600) to resolve all Fe isotopes from polyatomic  
 105 interferences (mainly ArO, ArOH, and ArN, see Weyer and Schwieters, 2003, for details).  
 106 Potential interferences from  $^{54}\text{Cr}$  on  $^{54}\text{Fe}$  and  $^{58}\text{Ni}$  on  $^{58}\text{Fe}$  were monitored at masses  $^{52}\text{Cr}$   
 107 and  $^{60}\text{Ni}$  and corrections to Fe isotope ratios were made according to the method described in  
 108 Schoenberg and von Blanckenburg (2005). In this study corrections made to the data are  
 109 insignificant compared to the analytical uncertainty, due to the low impurity levels of Cr and  
 110 Ni, i.e.,  $^{54}\text{Cr}/^{54}\text{Fe} < 0.005\%$  and  $^{58}\text{Ni}/^{58}\text{Fe} < 0.5\%$ . The sample-standard bracketing method  
 111 was used for mass bias correction (using IRMM-014 as bracketing standard), following the  
 112 measurement procedure and data acceptance criteria of Schoenberg & von Blanckenburg  
 113 (2005), and results are reported relative to the international reference material IRMM-014  
 114 using the delta notation:

$$\delta^{56}\text{Fe} = \left( \frac{[\text{}^{56}\text{Fe}/\text{}^{54}\text{Fe}]_{\text{sample}}}{[\text{}^{56}\text{Fe}/\text{}^{54}\text{Fe}]_{\text{standard}}} - 1 \right) \times 1000$$

116 Between 4 and 8 repeat measurements of each purified sample solution were  
 117 performed in 2 or 3 independent analytical sessions; the mean  $\delta$ -value of  $n$  replicates is  
 118 reported in Table 1 together with the 95% confidence interval ( $2\text{SE} = t \cdot \text{SD}/\sqrt{n}$ , with  $t =$   
 119 correction factor for small numbers of  $n$  from Student's  $t$ -distribution at 95% probability). For  
 120 data quality control, measurement accuracy and precision was assessed by repeated analyses  
 121 of an in-house working standard (HanFe: pure Fe solution used as control standard) in each  
 122 analytical session, and four aliquots of the reference material IRMM-014 ( $\delta^{56}\text{Fe} \equiv 0 \text{‰}$ ) were  
 123 independently processed through the same chromatographic separation protocol as the  
 124 samples. The uncertainty associated with the Fe separation and isotope analysis of IRMM-14  
 125 with  $\delta^{56}\text{Fe} = -0.03 \pm 0.05\%$  ( $2\sigma = 2$  standard deviation of the mean) and  $\delta^{57}\text{Fe} = -0.04 \pm$   
 126  $0.08\%$  ( $2\sigma$ ) agrees well with the mass spectrometric repeatability estimated over the course of  
 127 this study from the HanFe standard with  $\delta^{56}\text{Fe} = +0.27 \pm 0.05\%$  ( $2\sigma$ ,  $n=59$ ) and  $\delta^{57}\text{Fe}$  of

128  $+0.39 \pm 0.08\%$  ( $2\sigma$ ), and from the dataset of the 18 investigated chiton teeth samples ( $\sum n_i =$   
129 91 measured  $\delta$ -values) according to  $2 \cdot \sqrt{\{[\sum (x_i - x_{j-mean})^2] / [\sum (n_{i,j} - 1)]\}}$ , for the  $j^{\text{th}}$  chiton  
130 sample having a mean isotope composition  $x_{j-mean}$  determined from  $i$  replicate analyses  $x_i$ ,  
131 yielding  $\pm 0.05$  ( $2\sigma$ ) and  $\pm 0.08$  ( $2\sigma$ ) for  $\delta^{56}\text{Fe}$  and  $\delta^{57}\text{Fe}$ , respectively. Hence, the overall  
132 uncertainty estimate of the reported  $\delta^{56}\text{Fe}$  and  $\delta^{57}\text{Fe}$  values is  $\pm 0.05\%$  ( $2\sigma$ ) and  $\pm 0.08\%$   
133 ( $2\sigma$ ), respectively.

134

### 135 **3. RESULTS AND DISCUSSION**

#### 136 **3.1 Fe isotopic measurements in chiton teeth**

137 The  $\delta^{56}\text{Fe}$  values measured in the samples cover a wide range, varying from  $-1.90\%$  to  $0.00\%$   
138 (Figure 2). Although the overall range is quite large, the chiton specimens from each of the  
139 different regions cluster reasonably close together, with each chiton group possessing a  
140 distinct isotopic composition: *Chiton tuberculatus* from the sub-tropical north Atlantic  
141 (Bermuda) has a mean Fe isotope signature of  $\delta^{56}\text{Fe} = -0.23 \pm 0.32\%$  ( $2\sigma$ , 3 specimens),  
142 while the value for *Tonicella marmorea* from the North Atlantic (Grand Manan Island, New  
143 Brunswick, Canada) is  $-1.10\%$ . *Chiton stokesi* from the south Pacific (Panama) has a mean  
144  $\delta^{56}\text{Fe}$  value of  $-1.09 \pm 0.44\%$  ( $2\sigma$ , 5 specimens), while *Tonicella lineata* and *Mopalia*  
145 *muscosa* from the north Pacific (Puget Sound, Washington) possess mean  $\delta^{56}\text{Fe}$  values  
146 of  $-0.65 \pm 0.26\%$  ( $2\sigma$ , 8 specimens) and  $-1.47 \pm 0.98\%$  ( $2\sigma$ , 5 specimens), respectively,

147       Such large variation in isotopic signatures between the chitons in the different  
148 locations might be expected given the widely varying  $\delta^{56}\text{Fe}$  values reported for dissolved Fe  
149 (filtered  $<0.45 \mu\text{m}$ ) in seawater in different oceans. Isotopically heavy values in  $\delta^{56}\text{Fe}$  from  
150  $+0.01\%$  to  $+0.58\%$  have been measured at different locations in the Pacific Ocean (Lacan et  
151 al., 2010; Radic et al., 2011). At different depths too within the water column, significant  
152 variations in Fe isotope compositions have been reported in the Pacific Ocean: in the San

153 Pedro Basin in the North Pacific,  $\delta^{56}\text{Fe}$  values ranged from 0.00‰ at the surface to extremely  
154 negative values of -1.82‰ at a depth of 900 m. Large variations have also been reported in  
155 the Atlantic Ocean:  $\delta^{56}\text{Fe}$  values in the range from -0.14‰ to +0.23‰ have been reported for  
156 the Atlantic Section of the Southern Ocean (Lacan et al., 2008, 2010), while values of -0.13‰  
157 to 0.27‰ have been measured in the South East Atlantic (Lacan et al., 2010); in the North  
158 Atlantic  $\delta^{56}\text{Fe}$  values varying between +0.30‰ to +0.71‰ have been reported in some studies  
159 (John and Adkins, 2010; John and Adkins, 2012; Lacan et al., 2010), while off the north-  
160 eastern coast of North America isotopic signatures in the range -0.90‰ to +0.10‰ have also  
161 been reported (Rouxel & Auro, 2010). Such geographical dependence of seawater isotopic  
162 signatures is generally thought to be due to changes in the balance of different inputs and the  
163 influence of utilisation of Fe as a nutrient by marine organisms (e.g, Radic et al., 2011).  
164 Negative seawater values could be due to dissimilatory iron reduction or high local flux from  
165 continental runoff flux (Anbar & Rouxel, 2007), while positive values have been interpreted  
166 as indicative of non reductive dissolution of sediments (Radic et al., 2011).

167 Seawater samples taken at the same site and time of chiton sampling were not  
168 available for Fe isotope analyses in this preliminary study. However, to allow a first-order  
169 assessment of biological fractionation during Fe uptake from seawater, we compare our data  
170 with published data for Fe isotopes of dissolved Fe from surface or shallow seawater  
171 measured at locations as close as possible to the chiton sampling sites (Figure 2). For the three  
172 regions for which seawater Fe isotope values are reported (the north Atlantic, the south  
173 Atlantic, and the north Pacific),  $\delta^{56}\text{Fe}$  of dissolved Fe in surface seawater is more positive  
174 than the Fe in chiton teeth: the difference in  $\delta^{56}\text{Fe}$  values between seawater and chiton teeth  
175 ( $\Delta^{56}\text{Fe}_{\text{sw-chiton}} = \delta^{56}\text{Fe}_{\text{seawater}} - \delta^{56}\text{Fe}_{\text{chiton teeth}}$ ) at the different locations ranges from 0.28‰ to  
176 1.14‰. Thus, overall, Fe in chiton teeth would seem to be isotopically lighter than Fe in  
177 seawater, suggesting that fractionation processes determine the Fe isotope signatures in chiton

178 teeth. In the following sections we discuss 3 possible fractionation mechanisms controlling Fe  
179 isotope fractionation in chiton teeth, and these pathways are summarized schematically in  
180 Figure 3.

181

### 182 **3.2 Physiologically-controlled Fe isotope fractionation**

183 One of the possible mechanisms leading to differences between isotopic values in bulk  
184 seawater and those in chiton teeth could be associated with the mode of biomineralization  
185 within the chitons. In addition to magnetite ( $\text{Fe}_3\text{O}_4$ ), chiton radula contain other Fe minerals,  
186 including goethite ( $\alpha\text{-FeOOH}$ ), lepidocrocite ( $\gamma\text{-FeOOH}$ ), and ferrihydrite ( $\text{Fe}_2\text{O}_3 \cdot 0.5\text{H}_2\text{O}$ )  
187 (see Brooker and Shaw, 2012, and references therein). To form these minerals, iron originates  
188 as ferritin in the haemolymph and is delivered to the superior epithelial cells of the radula sac  
189 (Shaw et al., 2009). At a later stage, the ferritin is transferred to an organic matrix where it is  
190 deposited as ferrihydrite (Kim et al., 1989; Brooker et al., 2003). Despite the recent efforts in  
191 materials science to better understand Fe biomineralization (e.g, Weaver et al., 2010; Xiao  
192 and Yang, 2012), the precise mechanism by which the ferrihydrite precursor is transformed to  
193 magnetite remains undetermined. However, this transformation must involve a transition from  
194 an Fe(III) mineral (ferrihydrite) to a mineral that contains both Fe(II) and Fe(III) (magnetite).  
195 Moreover, changes in redox state can cause relatively large equilibrium Fe isotope  
196 fractionations (Wu et al, 2011; Frierdich et al., 2014); for example formation of magnetite  
197 from aqueous Fe(II) at 22°C leads to a mineral isotopic signature that is around  $\sim 1.6\text{‰}$   
198 heavier, while precipitation of ferrihydrite from aqueous Fe(II) leads to mineral isotopic  
199 values that are between 2.5‰ to 3.2‰ heavier. Mineralogical compositions in chiton teeth  
200 vary from species to species (Lowenstam and Weiner, 1989), and different proportions of the  
201 Fe bearing minerals could therefore result in distinct overall isotopic signatures. In future  
202 studies, precise measurements of Fe isotopes in the various mineralogical phases using new

203 techniques, such as laser ablation MC-ICP-MS, could be used to assess fractionation  
204 processes during biomineralization.

205

### 206 **3.3 Diet-controlled fractionation**

207 Another potential mechanism affecting the isotopic values in the chiton teeth is the direct  
208 ingestion of Fe that is isotopically distinct to iron in seawater. The main source of food for  
209 chitons is red and green algae; both types of algae are known to fractionate oxygen and  
210 carbon isotopes (Anderson and Arthur, 1983), and it is feasible that Fe isotopes might also be  
211 fractionated during uptake by algae. Algae contain high concentrations of Fe (e.g., García-  
212 Casal et al., 2007), having developed a range of strategies for creating bioavailable Fe(II)  
213 from low solubility Fe(III) species, including the use of siderophores that facilitate  
214 photochemical redox cycling (e.g., Amin et al., 2009). Uptake mechanisms produce strong  
215 fractionations in terrestrial plants (von Blanckenburg et al., 2009; Guelke-Stelling and von  
216 Blanckenburg, 2012), and if enough Fe(II) is available, the light isotope may be preferentially  
217 absorbed, producing a light  $\delta^{56}\text{Fe}$  signal which could depend on algal type.

218 Curiously, the isotopic values measured in the two chiton species from Puget Sound  
219 (Washington, USA) seem to have distinct values. The range in  $\delta^{56}\text{Fe}$  values obtained from 5  
220 individual specimens of *Tonicella lineata* is from -0.83‰ to -0.45‰ (mean  $\delta^{56}\text{Fe} = -0.65 \pm$   
221  $0.26\%$ ,  $2\sigma$ ); in contrast, more negative  $\delta^{56}\text{Fe}$  values ranging from -1.90‰ to -0.94‰ (mean  
222  $\delta^{56}\text{Fe} = -1.47 \pm 0.98\%$ ,  $2\sigma$ ) were found for the 3 specimens of *Mopalia muscosa* (Figure 2).  
223 As one of the important differences between the two species is their contrasting diets (*T.*  
224 *lineata* predominantly feeds on red algae, while *M. muscosa* has a diet that includes both  
225 green and red algae (Booolootian, 1964; Demopoulos, 1975), food sources could account for the  
226 different isotopic compositions. Furthermore, the variance associated with the  $\delta^{56}\text{Fe}$  signature  
227 for *M. muscosa* is much higher than the variance for *T. lineata*, which would seem to be

228 consistent with the observation that chitons from the eulittoral zone (intertidal zone), such as  
229 *M. muscosa*, have less specific feeding habits, often ingesting both red and green algae and  
230 even animal matter (Booolootian, 1964; Morris et al., 1980).

231 While isotopic analyses of the different algal types would help evaluate the role of diet  
232 in determining the chitons' isotopic signatures, samples were not available for analysis in the  
233 current study. However, biological fractionation by algae is supported by an Fe isotope  
234 difference measured between phytoplankton and seawater, where an isotopic fractionation of  
235 about 0.25‰ favouring light isotopes was suggested to occur during uptake by phytoplankton  
236 (Bergquist and Boyle, 2006; Radic et al., 2011). Thus, the observed isotopic differences  
237 between seawater and chiton teeth could be at least be partially controlled by algal-mediated  
238 fractionation.

239 We note here that direct ingestion of Fe from rocky substrates with different isotopic  
240 signatures could also affect the chiton teeth (Lowenstam and Kirschvink, 1996). However, the  
241 Fe isotope composition of crustal igneous rocks is relatively restricted, ranging from about  
242 0‰ to +0.4‰ in  $\delta^{56}\text{Fe}$  (e.g., Beard et al., 2003, Poitrasson and Freydier, 2005) with an  
243 average igneous rock composition of  $0.1 \pm 0.1\%$  ( $2\sigma$ ) (Beard et al., 2003). Modern marine  
244 sediments, such as terrigenous sediments, turbidite clays, and volcanoclastites, as well as  
245 altered oceanic crust, also have a restricted range of Fe isotope compositions clustered around  
246 the average igneous  $\delta^{56}\text{Fe}$  value, with variations of less than 0.3‰ (e.g., Beard et al., 2003;  
247 Rouxel et al., 2003; Fantle and DePaolo, 2004), consistent with the homogeneous Fe-isotope  
248 composition found in loess and aerosols (Zhu et al. 2000). Thus, Fe derived from rocky  
249 substrates is unlikely to account for the very light Fe isotope values we measured, although  
250 confirming this would have required *in situ* sampling that was beyond the constraints of this  
251 preliminary study.

252

### 253 **3.4 Environmentally-controlled fractionation**

254 Environmental conditions in the eulittoral and sublittoral zones are significantly different, and  
255 they could exert an additional control on the isotopic pools of bioavailable Fe. In near-surface  
256 coastal seawater, dissolved bioavailable Fe(II) is thought to be produced by the photo-  
257 reduction of Fe(III) nanoparticles and complexes (e.g., Johnson et al., 1994; Barbeau et al.,  
258 2000; Barbeau, 2006; Fan, 2008). Measurements of seawater indicate that Fe(II)  
259 concentrations decrease significantly with depth in the top 10 m of the water column (e.g.,  
260 Shaked, 2008), suggesting that photoreduction of Fe(III) to Fe(II) may be more effective in  
261 the shallower eulittoral zone than in the deeper sublittoral zone. Importantly, experiments  
262 have shown that the reductive dissolution of Fe-oxides produces isotopically light Fe(II) (e.g.,  
263 Wiederhold et al., 2006; Beard et al., 2010), and photoreduction might be expected to produce  
264 bioavailable Fe(II) in seawater that possesses negative  $\delta^{56}\text{Fe}$  values. Moreover, differences in  
265 levels of photoreduction could produce bioavailable Fe(II) with light  $\delta^{56}\text{Fe}$  values in the  
266 eulittoral zone and heavier isotopic values in the deeper sublittoral zone. Importantly, such a  
267 mechanism is consistent with the measurements of different chiton species from Puget Sound:  
268 Fe isotopes in *M. Muscosa* from the eulittoral zone are indeed lighter than those in *T. lineata*  
269 from the sublittoral zone. Thus, the different isotopic ratios measured in the two species may  
270 reflect different water depths and levels of photoreduction in the near shore environment.

271

### 272 **CONCLUDING REMARKS**

273 In this paper, we report on the Fe isotopic compositions of chiton radula from different marine  
274 locations in the Pacific and Atlantic oceans. We found a large variation in  $\delta^{56}\text{Fe}$  values  
275 between the different locations, suggesting that the isotopic compositions may in part be  
276 controlled by variations in the local isotopic source signature due to changes in the relative  
277 balance of inputs from dissimilatory iron reduction, continental runoff, and non reductive  
278 dissolution of sediments. However, the distinct signatures recorded from two different species

279 analysed from Puget Sound, USA, suggest that Fe isotopes could be influenced by three main  
280 processes: (i) physiologically-controlled processes within the chitons that cause species  
281 dependent fractionation; (ii) diet-controlled variability resulting from different Fe isotope  
282 fractionation in the red and green algal food sources; (iii) environmentally-controlled  
283 fractionation that leads to variation in the isotopic signatures of bioavailable Fe in the  
284 different tidal zones.

285         Clearly the dataset presented in the current study possesses a number of limitations.  
286 Firstly, the number of chitons in our study is relatively small, a fact that complicates the  
287 interpretation of the results. In addition, although a dataset of published Fe isotope values for  
288 seawater exists, no Fe isotope data are available for algae and seawater from the exact  
289 locations from which the chiton specimens were collected; moreover, even if values were to  
290 be obtained for the present day, it is unclear how relevant such data would be for the samples  
291 in this study that were collected decades ago. In view of such constraints, our study must be  
292 regarded as a first attempt to tackle the complexities of Fe isotope fractionation in marine  
293 invertebrates, and our findings regarding the Fe isotope fractionation mechanisms are  
294 therefore preliminary. To determine the relative significance of the pathways controlling Fe  
295 isotopic signatures, a far more extensive sampling campaign – involving in-situ measurements  
296 of water, rock substrates, algae, and chitons – would be necessary.

297         Despite the limited dataset, the present study nevertheless yields a number of  
298 important conclusions. Although the results suggest that Fe-isotopes in bio-minerals do not  
299 necessarily record oceanic values, iron-concentrating organisms such as chitons  
300 (polyplacophora) and even limpets (archeogastropods) – which have teeth containing goethite  
301 (Lowenstam, 1962b) – could still record the signature of dissolved bioavailable Fe, and  
302 provide information concerning Fe biogeochemical cycling in near shore environments.  
303 Furthermore, in a similar way to oxygen and nitrogen isotopes, Fe isotopes could be used to  
304 distinguish between the primary sources of Fe in the diets of different organisms, serving as

305 an additional tool with which to probe ecological systems. Although the difficulties associated  
306 with identifying Fe-biominerals in the fossil record (Chang and Kirschvink, 1989) currently  
307 limit their potential usefulness in reconstructing past conditions, further documentation of Fe  
308 isotopes in seawater, algae, and higher organisms is expected to help track the present-day  
309 pathways and sources of Fe in marine environments.

310

### 311 **ACKNOWLEDGMENTS**

312 We thank the associate editor, an anonymous reviewer, and Damien Cardinal for their  
313 constructive comments. Douglas Eernisse and Yaela Shaked are also thanked for their helpful  
314 advice. SE would like to thank the German Israel Foundation for Scientific Research and  
315 Development for generous financial support via their Young Scientists' Program. In addition,  
316 we are grateful to Eric Lazo-Wasem and Lourdes Rojas for providing access to the Yale  
317 Peabody Museum invertebrate zoological collection.

318

319 **REFERENCES**

- 320 Anbar AD, Rouxel OM (2007) Metal stable isotopes in paleoceanography. *Annu Rev Earth*  
321 *Planet Sci* 35:717-746.
- 322 Anderson, T.F. and M.A., Arthur, 1983. Stable Isotopes of Oxygen and Carbon and Their  
323 Application to Sedimentologic and Paleoenvironmental Problems. In: *Stable Isotopes in*  
324 *Sedimentary Geology*, Arthur, M.A., T.F. Anderson, I.R. Kaplan, J. Veizer and L. Land  
325 (Eds.). SEPM, Short Course Notes Vol 10, Georgia, pp: 1-151.
- 326 Amin SH, Green DH, Hart MC, Küpper FC, Sunda WG, Carrano CJ (2009) Photolysis of  
327 iron–siderophore chelates promotes bacterial–algal mutualism. *Proc Natl Acad Sci*  
328 106:17071- 17076.
- 329 Barbeau, K (2006) Photochemistry of organic iron(III) complexing ligands in oceanic  
330 systems. *Photochem Photobiol* 82:1505-1516.
- 331 Barbeau K, Moffett J (2000) Laboratory and field studies of colloidal iron oxide dissolution  
332 as mediated by phagotrophy and photolysis. *Limnol Oceanogr* 45:827–835.
- 333 Beard, BL, Johnson CM, Von Damm, KL, Poulson, RL (2003a). Iron isotope constraints on  
334 Fe cycling and mass balance in the oxygenated earth's oceans. *Geology* 31:629-632.
- 335 Beard BL, Johnson CM, Skulan JL, Nealson KH, Cox L, Sun H (2003b) Application of Fe  
336 isotopes to tracing the geochemical and biological cycling of Fe. *Chem Geol* 195:87-118.
- 337 Beard, BL, Handler, RM, Scherer, MM, Wu, L, Czaja, AD, Heimann, A, Johnson, CM (2010)  
338 Iron isotope fractionation between aqueous ferrous iron and goethite. *Earth Planet. Sci.*  
339 *Letts.* 295, 241-250.
- 340 Bergquist BA, Boyle EA (2006) Iron isotopes in the Amazon River system: Weathering and  
341 transport signatures. *Earth Planet Sci Lett* 248:39–53.
- 342 Boolootian RA (1964) On growth, feeding and reproduction in the chiton *Mopalia muscosa* of  
343 Santa Monica Bay Helgoland. *Mar Res* 11:186-199.

344 Brantley SL, Liermann LJ, Guynn RL, Anbar A, Icopini GA, Barling J (2004). Fe isotopic  
345 fractionation during mineral dissolution with and without bacteria. *Geochim*  
346 *Cosmochim Acta*, 68:3189-3204.

347 Brooker LR, Lee AP, Macey DJ, van Bronswijk W, Webb J (2003) Multiple-front iron-  
348 mineralisation in chiton teeth (*Acanthopleura echinata*: Mollusca: Polyplacophora). *Mar*  
349 *Biol* 142:447–454.

350 Brooker LR, Shaw JA (2012) The chiton radula: a unique model for biomineralization  
351 studies, In: Seto J (ed) *Advanced Topics in Biomineralization*, pp 65-84.

352 Chang, SR, and Kirschvink JL (1989) Magnetofossils, the magnetization of sediments, and  
353 the evolution of magnetite biomineralization. *Annu. Rev. Earth Planet. Sci.* 17:169-195.

354 Coale KH, Fitzwater SE, Gordon RM, Johnson KS, Barber RT (1996) Control of community  
355 growth and export production by upwelled iron in the equatorial Pacific Ocean. *Nature*  
356 379:621 - 624.

357 Crosby HA, Roden EE, Johnson CM, Beard BL (2007) The mechanisms of iron isotope  
358 fractionation produced during dissimilatory Fe(III) reductions by *Shewanella putrefaciens*  
359 and *Geobacter sulfurreducens*. *Geobiology* 8:169–189.

360 De Baar HJW, De Jong JTM, Bakker DCC, Löscher BM, Veth C, Bathmann U, Smetacek V  
361 (1995) Importance of iron for plankton blooms and carbon dioxide drawdown in the  
362 Southern Ocean. *Nature* 373:412 – 415.

363 Demopoulos, DA (1975) Diet, activity and feeding in *Tonicella lineate* (Wood, 1815). *Veliger*,  
364 18:42-46.

365 Fan, SM (2008) Photochemical and biochemical controls on reactive oxygen and iron  
366 speciation in the pelagic surface ocean. *Mar Chem* 109:152-164.

367 Fantle MS, DePaolo DJ (2004) Iron isotopic fractionation during continental weathering.  
368 *Earth Planet Sci Lett* 228: 547-562.

369 Frierdich, AJ, Beard, BL, Scherer, MM, Johnson, CM (2014) Determination of the Fe(II)<sub>aq</sub>-  
370 magnetite equilibrium iron isotope fractionation factor using the three-isotope method and  
371 a multi-direction approach to equilibrium. *Earth Planet Sci Letts* 391: 77-86.

372 García-Casal MN, Pereira AC, Leets I, Ramírez J, Quiroga MF (2007) High iron content and  
373 bioavailability in humans from four species of marine algae. *J Nutr* 137:2691-2695.

374 Glynn, P. W. (1970). *On the Ecology of the Caribbean Chitons Acanthopleura Granulata*  
375 *Gmelin and Chiton Tuberculatus Linni: Density, Mortality, Feeding, Reproduction, and*  
376 *Growth. Smithsonian Institution Press.*

377 Guelke-Stelling M, von Blanckenburg F (2012) Fe isotope fractionation caused by  
378 translocation of iron during growth of bean and oat as models of strategy I and II plants.  
379 *Plant Soil* 352:217-231.

380 Homoky, WB, John, SG, Conway, TM, Mills, RA (2013). Distinct iron isotopic signatures  
381 and supply from marine sediment dissolution. *Nat. Commun.* 4, 2143.

382 Hotz K, Augsburg H, Walczyk T (2011) Isotopic signatures of iron in body tissues as a  
383 potential biomarker for iron metabolism. *J Anal Atom Spec* 26:1347-1353.

384 John SG, Adkins JF (2010) Analysis of dissolved iron isotopes in seawater. *Mar Chem*  
385 119:65-76.

386 John, SG and Adkins, JF (2012) The vertical distribution of iron stable isotopes in the North  
387 Atlantic near Bermuda. *Global Biogeochem. Cycles*, 26, GB2034,  
388 doi:0.1029/2011GB004043.

389 Johnson KS, Coale KH, Elrod VA, Tindale NW (1994) Iron photochemistry in seawater from  
390 the equatorial Pacific. *Mar Chem* 46:319-334.

391 Johnson CM, Roden EE, Welch SA, Beard BL (2005) Experimental constraints on Fe isotope  
392 fractionation during magnetite and Fe carbonate formation coupled to dissimilatory  
393 hydrous ferric oxide reduction. *Geochim Cosmochim Acta* 69:963-993.

394 Johnson CM, Beard BL, Roden EE (2008) The iron isotope fingerprints of redox and  
395 biogeochemical cycling in the modern and ancient Earth. *Annu Rev Earth Planet Sci*  
396 36:457- 493.

397 Kim KS, Macey DJ, Webb J, Mann S (1989) Iron mineralization in the radula teeth of the  
398 chiton *Acanthopleura hirtosa*. *Proc R Soc Lond B* 237:335-346.

399 Lacan F, Radic A, Jeandel C, Poitrasson F, Sarthou G, Pradoux C, Freydier R (2008)  
400 Measurement of the isotopic composition of dissolved iron in the open ocean. *Geophys*  
401 *Res Lett* 35:L24610, doi:10.1029/2008GL03584.

402 Lacan F, Radic A, Labatut M, Jeandel C, Poitrasson F, Sarthou G, Pradoux C, Chmeleff J,  
403 Freydier R (2010) High-precision determination of the isotopic composition of dissolved  
404 iron in iron depleted seawater by double spike multicollector-ICPMS. *Anal Chem* 82:7103-  
405 7111.

406 Lowenstam, HA (1962a) Magnetite in denticle capping in recent chitons (polyplacophora).  
407 *Geol Soc Am Bull* 73: 435-438.

408 Lowenstam, HA (1962b). Goethite in radular teeth of recent marine gastropods. *Science*  
409 137:279-280.

410 Lowenstam, HA, Kirschvink, JL (1996) Iron Biomineralization - A Geobiological  
411 Perspective. In: Kirschvink, JL, Jones DS, McFadden BJ (eds) *Magnetite*  
412 *Biomineralization and Magnetoreception in Organisms*, New York, N.Y., Plenum Press. 5:  
413 3-15.

414 Lowenstam, HA and Weiner S (1989). *On Biomineralization*. Oxford, Oxford University  
415 Press.

416 Martin JH, Gordon M, Fitzwater SE (1990) Iron in Antarctic water. *Nature* 345:156-158.

417 Matthews A, Zhu XK, O’Nions RK (2001) Kinetic iron stable isotope fractionation between  
418 iron (II) and iron (III) complexes in solution. *Earth Planet Sci Lett* 192:81-92.

419 Matthews A, Morgans-Bell HS, Emmanuel S, Jenkyns HC, Erel Y, Halicz L (2004) Controls  
420 on iron-isotope fractionation in organic-rich sediments (Kimmeridge Clay, Upper Jurassic,  
421 southern England). *Geochim Cosmochim Acta* 68:3107-3123.

422 Matthews A, Emmanuel S, Levi L, Gvirtzman H, Erel Y (2008) Kinetic fractionation of Fe  
423 isotopes during transport through a porous quartz medium. *Geochim Cosmochim Acta*  
424 72:5908-5919.

425 Morris, RH, Abbott, DP, Haderlie, EC (1980). *Intertidal Invertebrates of California*. Stanford  
426 University Press.

427 Poitrasson F, Freydier R (2005) Heavy iron isotope composition of granites determined by  
428 high resolution MC-ICP-MS. *Chem Geol* 222:132–147.

429 Radic A, Lacan F, Murray JW (2011) Iron isotopes in the seawater of the equatorial Pacific  
430 Ocean: New constraints for the oceanic iron cycle. *Earth Planet Sci Lett* 306:1-10.

431 Rouxel O, Dobbek N, Ludden J, Fouquet Y (2003) Iron isotope fractionation during oceanic  
432 crust alteration. *Chem Geol* 202:155-182.

433 Rouxel OJ, Auro M (2010) Iron isotope variations in coastal seawater determined by  
434 multicollector ICP-MS. *Geostand Geoanal Res* 34:135-144.

435 Schoenberg R, von Blanckenburg F (2005) An assessment of the accuracy of stable Fe  
436 isotope ratio measurements on samples with organic and inorganic matrices by high-  
437 resolution multicollector ICP-MS. *Int J Mass Spec* 242:257-272.

438 Severmann S, Johnson CM, Beard BL, McManus J (2006) The effect of early diagenesis on  
439 the Fe isotope compositions of pore waters and authigenic minerals in continental margin  
440 sediments. *Geochim Cosmochim Acta* 70:2006-2022.

441 Shaked, Y. (2008) Iron redox dynamics in the surface waters of the Gulf of Aqaba, Red  
442 Sea. *Geochim Cosmochim Acta*, 72, 1540-1554.

443 Sharma M, Polizatto M, Anbar AD (2001) Iron isotopes in hot springs along the Juan de Fuca  
444 Ridge. *Earth Planet Sci Lett* 194:39-51.

445 Shaw JA, Macey DJ, Brooker LR, Stockdale EJ, Saunders M, Clode PL (2009) The chiton  
446 stylus canal: An element delivery pathway for tooth cusp biomineralization. *J Morph*  
447 270:588-600.

448 Staubwasser M, von Blanckenburg F, Schoenberg R (2006) Iron isotopes in the early marine  
449 diagenetic iron cycle. *Geology* 34:629-632.

450 Teutsch N, Von Gunten U, Porcelli D, Cirpka OA, Halliday AN (2005) Adsorption as a cause  
451 for iron isotope fractionation in reduced groundwater. *Geochim Cosmochim Acta*  
452 69:4175–4185.

453 Towe, KM and Lowenstam HA (1967) Ultrastructure and development of iron mineralization  
454 in the radular teeth of *Cryptochiton stelleri* (Mollusca). *J Ultrastruct Res* 17:1-13.

455 von Blanckenburg F, von Wirén N, Guelke M, Weiss D, Bullen T (2009) Fractionation of  
456 metal stable isotopes by higher plants. *Elements* 5:375-380.

457 Walczyk T, von Blanckenburg F (2002) Natural iron isotope variations in human blood.  
458 *Science* 295:2065-2066.

459 Weaver JC, Wang Q, Miserez A, Tantuccio A, Stromberg R, Bozhilov KN, Maxwell P, Nay  
460 R, Heier ST, DiMasi E, Kisailus D (2010) Analysis of an ultra hard magnetic biomineral in  
461 chiton radular teeth. *Materials Today* 13: 42-52.

462 Welch SA, Beard BL, Johnson CM, Braterman PS (2003) Kinetic and equilibrium Fe isotopic  
463 fractionation between aqueous Fe(II) and Fe(III). *Geochim Cosmochim Acta* 67:4231-  
464 4250.

465 Weyer S, Schwieters JB (2003) High precision Fe isotope measurements with high mass  
466 resolution MC-ICPMS. *Int J Mass Spec* 226:355-368.

467 Wiederhold JG, Kraemer SM, Teutsch N, Borer PM, Halliday AN, Kretzschmar R (2006)  
468 Iron isotope fractionation during proton-promoted, ligand-controlled, and reductive  
469 dissolution of goethite. *Environ Sci Technol* 40:3787-3793.

470 Wu, L, Beard, BL, Roden, EE, Johnson, CM (2011) Stable iron isotope fractionation between  
471 aqueous Fe (II) and hydrous ferric oxide. *Environ. Sci. Technol.*, 45: 1847-1852.

472 Xiao J, Yang S (2012) Bio-inspired synthesis: Understanding and exploitation of the  
473 crystallization process from amorphous precursors. *Nanoscale* 4: 54-65.

474 Zhu XK, Guo Y, Williams RJP, O'Nions RK, Matthews A, Belshaw N, Canters GW, de Waal  
475 EC, Weser U, Burgess BK, Salvato B (2002) Mass fractionation of the transition metal  
476 isotopes. *Earth Planet Sci Lett* 200:47-62.

477 Zhu XK, O'Nions RK, Guo YL, Reynolds BC (2000) Secular variation of iron isotopes in  
478 North Atlantic Deep Water. *Science* 287: 2000-2002.

479

TABLE 1: SUMMARY OF ANALYSED CHITON SAMPLES.

Species	Individual specimens	Locality	Ecology	Specimen ID	$\delta^{56}\text{Fe}$ ‰	2SE ‰	$\delta^{57}\text{Fe}$ ‰	2SE ‰	<i>n</i>
<i>Tonicella lineata</i>	5	Puget Sound, WA, USA	Sublittoral,	YPM-12716-01	-0.57	0.04	-0.84	0.07	4
				red algae	YPM-12716-02	-0.73	0.05	-1.07	0.07
				YPM-12716-03	-0.56	0.05	-0.83	0.05	5
				YPM-12720-04	-0.54	0.04	-0.82	0.07	5
				YPM-12720-05	-0.83	0.05	-1.22	0.06	4
<i>Mopalia muscosa</i>	3	Puget Sound, WA, USA	Eulittoral,	YPM-12718-06	-1.58	0.04	-2.33	0.06	5
			green algae	YPM-12718-07	-1.90	0.02	-2.81	0.03	6
				YPM-12718-08	-0.94	0.04	-1.39	0.04	5
<i>Tonicella marmorea</i>	8	Grand Manan Island, New Brunswick, Canada	Sublittoral, red algae	YPM-12760-09	-1.10	0.05	-1.61	0.06	5
<i>Chiton stokessi</i>	5	Panama	Eulittoral,	YPM-5176-10	-1.11	0.03	-1.63	0.05	6
				green algae	YPM-5176-11	-1.26	0.01	-1.86	0.03
				YPM-5176-12	-0.73	0.04	-1.03	0.07	5
				YPM-5176-13	-1.29	0.06	-1.89	0.06	4
				YPM-5176-14	-1.06	0.05	-1.54	0.09	4
<i>Chiton tuberculatus</i>	3	Bermuda	Eulittoral,	YPM-12739-15	-0.38	0.01	-0.54	0.03	6
			green algae	YPM-12739-16a	0.00	0.05	0.00	0.09	4
				YPM-12739-16b	-0.28	0.02	-0.40	0.04	8
				YPM-12739-17	-0.28	0.05	-0.40	0.07	5

Iron isotope data are reported as permil deviation relative to the international reference material IRMM-014. Mean values of *n* replicate analyses of the same analyte solution are reported with their 95% confidence intervals ( $2SE = t \cdot SD/\sqrt{n}$ , with *t* = correction factor from Student's *t*-distribution at 95% probability). Uncertainties in  $\delta^{56}\text{Fe}$  and  $\delta^{57}\text{Fe}$  associated with the entire Fe isotope analytical procedure are estimated to be  $\pm 0.05$  ‰ ( $2\sigma$ ) and  $\pm 0.08$  ‰ ( $2\sigma$ ), respectively (see text).

Figure 1: (a) *Chiton tuberculatus* in the eulittoral zone, and (b) a radula sac containing the magnetite-capped teeth, indicated by the arrow. *C. tuberculatus* specimens are typically 14-80 mm in length (Glynn, 1970), and the one shown in (a) is approximately 50 mm long.

481 Figure 2: Fe isotope signatures of 18 chiton teeth analyses (grey circles). Analytical  
482 uncertainties in  $\delta^{56}\text{Fe}$  are smaller than the symbols. Data points encircled by the red dashed  
483 lines indicate chitons with a red-algae rich diet, while green dotted lines indicate a  
484 predominantly green algae diet. Note that the values for the chitons with a red-algae diet from  
485 Washington cluster close together; by contrast, chitons from the same location with a diet of  
486 green algae have a larger variance and a lighter isotopic signature. The single value for  
487 *Tonicella marmorea* from Grand Manan Island represents the average of 8 homogenized  
488 specimens. For comparison, the average for igneous rocks (Beard et al., 2003) is indicated by  
489 the vertical grey line, while the range of Fe isotope values reported in the literature for  
490 dissolved Fe in surface and shallow (< 75 m depth) seawater (Lacan et al., 2008, 2010; John  
491 and Adkins 2010, 2012; Rouxel and Auro, 2010; Radic et al., 2011) is represented by the  
492 solid blue band at the bottom. Blue squares are published surface seawater isotope analyses of  
493 dissolved Fe from locations as close to the chiton sampling sites as available data permits.  
494 Data reported by Rouxel and Auro, (2010) for three sites located off the north-eastern Atlantic  
495 coast of North America are (a) Vineyard Sound on Cape Cod, Massachusetts, USA (-0.82  
496 ‰); (b) Waquoit Bay on Cape Cod, Massachusetts, USA (-0.55 ‰); (c) Connecticut River  
497 estuary in Long Island Sound, Connecticut, USA (+0.04 ‰). These three sites are located  
498 within less than 150 km distance from each other, on average about 500 km south of the  
499 chiton sampling site at Grand Manan Island, New Brunswick, CA). Data for the North  
500 Atlantic (d) (+0.3 ‰; sampled about 100 km southeast from Bermuda, John and Adkins,  
501 2010; John and Adkins, 2012) are compared with the Bermuda chiton sampling site. The  
502 closest available coastal seawater Fe isotope data to compare with the Puget Sound chiton  
503 sampling site (Washington, USA) is from the San Pedro Basin (e) (0 ‰; John and Adkins,  
504 2010), which is located off the Atlantic coast near Los Angeles (California, USA), about 1500  
505 km south from Puget Sound.

Figure 3: Schematic pathways for isotope fractionation of iron present in seawater and different chiton species. Fractionation could occur during (a) physiologically-controlled biomineralization processes within the chitons; (b) fractionation during uptake by algae and subsequent ingestion; and (c) environmentally-controlled photoreductive dissolution of Fe complexes and nanoparticles in seawater. The mechanisms are not mutually exclusive and the signatures in the chiton teeth could reflect a combination of different pathways.

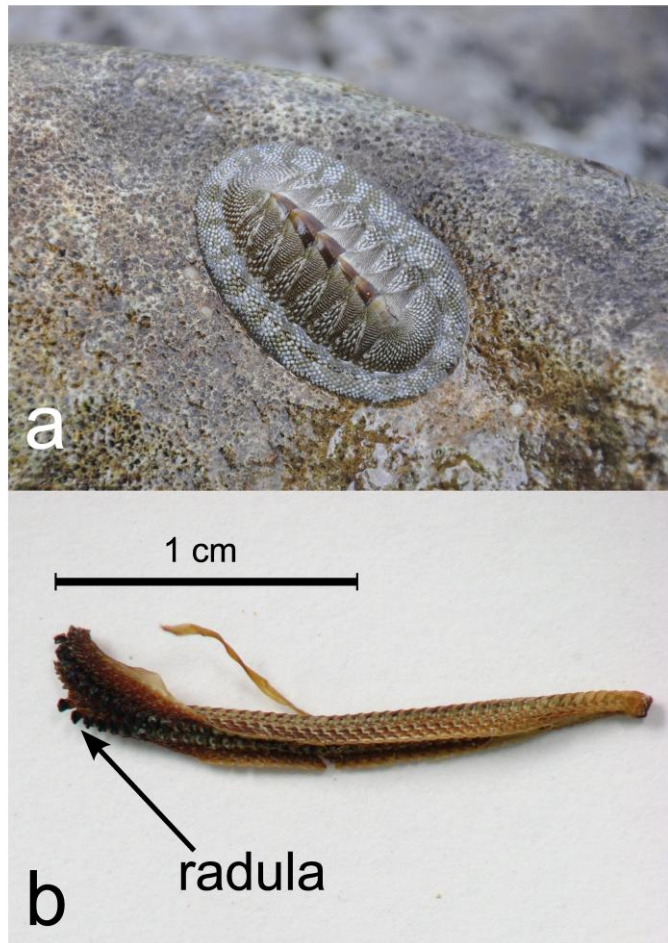


**Figure 1**

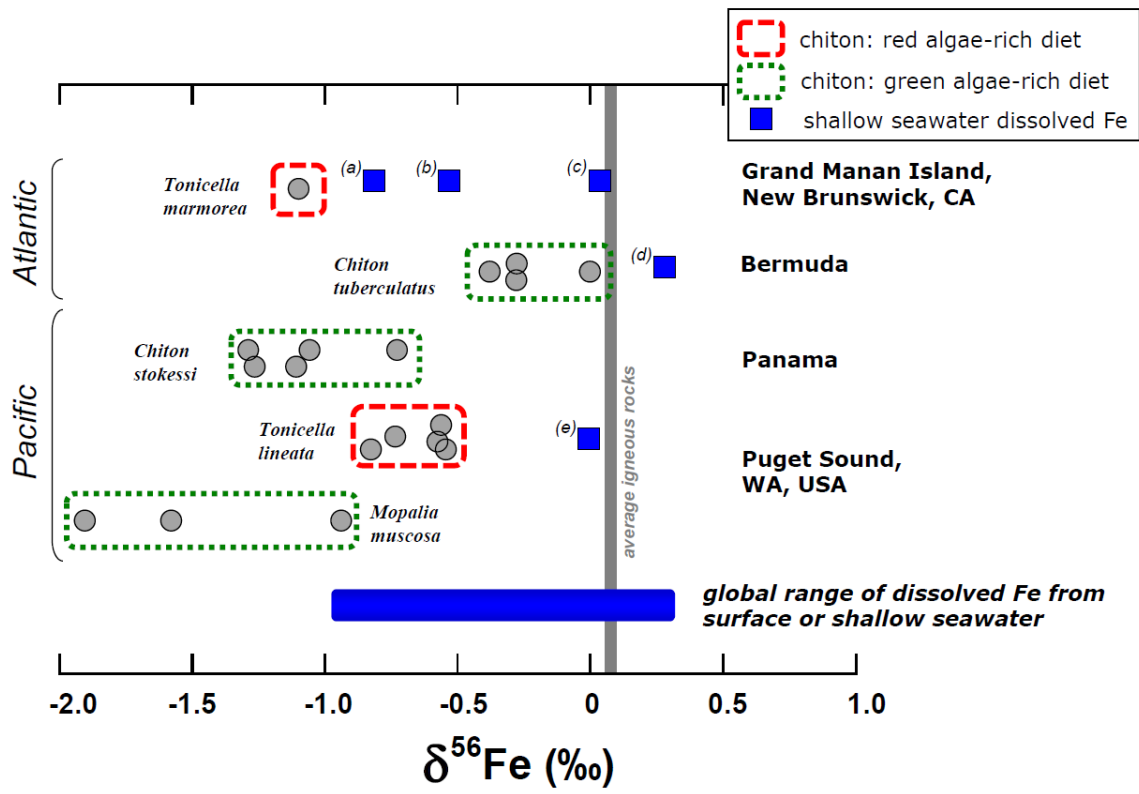


Figure 2

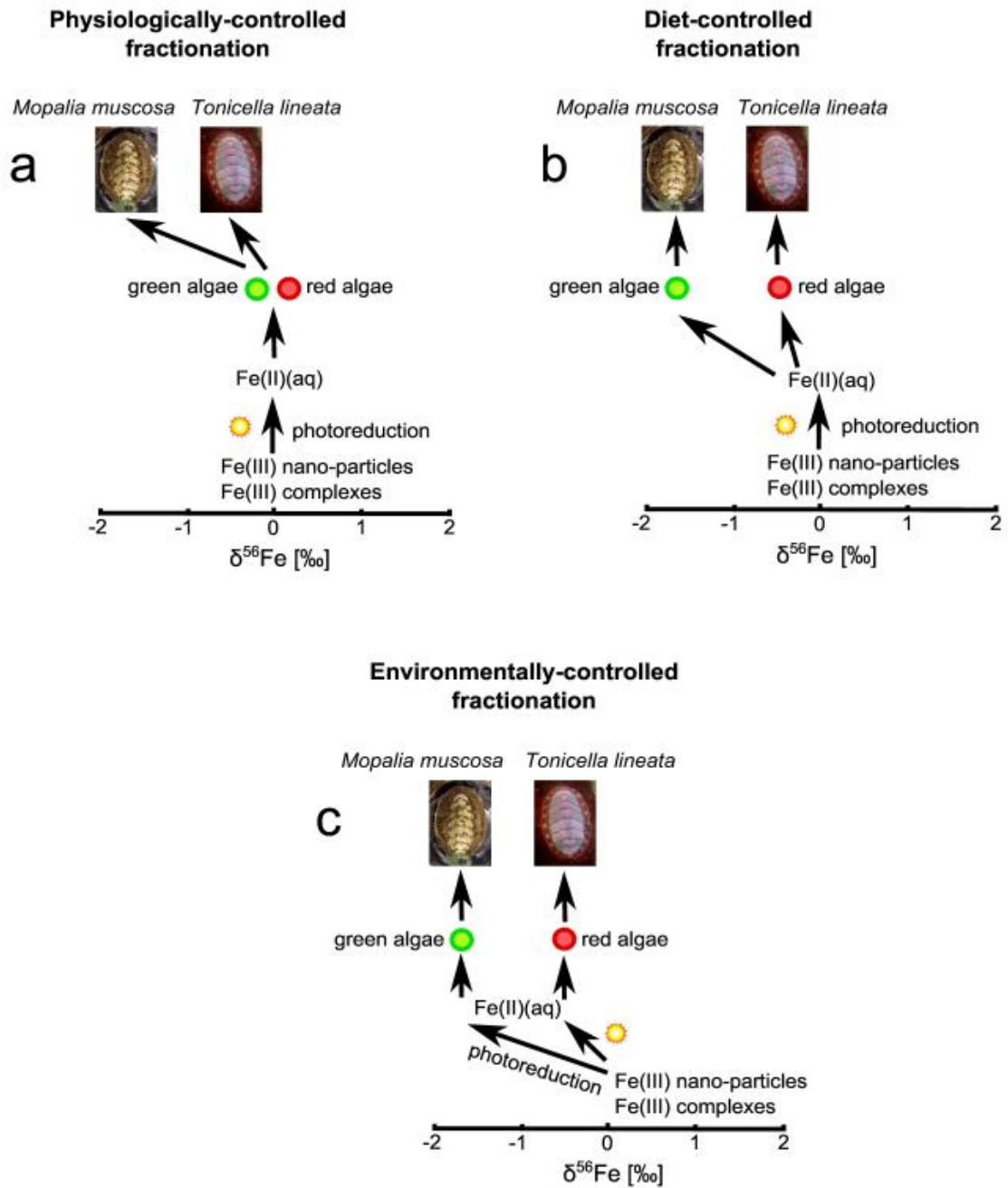


Figure 3